

tive stresses alternate over the unit cell. Because of the different stress states the evolution of σ_{yy} differs for the two configurations.

As stated earlier, the average stress changes with the volume percentage of large grains. In Figure 10 the maximum σ_{yy} stress is normalized against the average loading stress $\bar{\sigma}_{xx}$ at uniaxial strain of $\bar{\epsilon}_{xx} = 5\%$ and plotted against the volume percentage of large grains. As seen in the plot, initially the σ_{yy} stress increases as the percentage of large grains increases for the two configurations. But, eventually the σ_{yy} stress reaches a maximum value and the stress decreases. As stated earlier, the real material mostly consists of small grains, therefore, we normally have a material where an increased amount of large grains gives higher σ_{yy} stress. With this condition large grains are not wanted.

The positive σ_{yy} stress is due to different properties of the small and large grains, and even though the maximum σ_{yy} stress is only a fraction of the maximum von Mises effective stress, it can play an important role in the damage evolution in high-strength strip steel. The steel is often weaker in the thickness direction, due to the elongated microstructure. The transverse stresses may therefore be critical for initiation of delamination. The present studies indicate that the volume fraction of large grains should be kept as small as possible.

Three primary results can be concluded from this work.

- First, as the steel sheet is loaded by an average strain, $\bar{\epsilon}_{xx}$, concentrations of transverse stresses, σ_{yy} , arise in the vicinity of the tip of the elliptical area. These stresses can reach about a quarter of the maximum von Mises effective stress, and can thereby be the source of delaminations, since the high-strength steel is weaker in the thickness direction due to the elongated microstructure.
- Secondly, the simple rule of mixtures can be used to describe the macroscopic behavior of the model containing large grains forming elliptical shaped colonies.

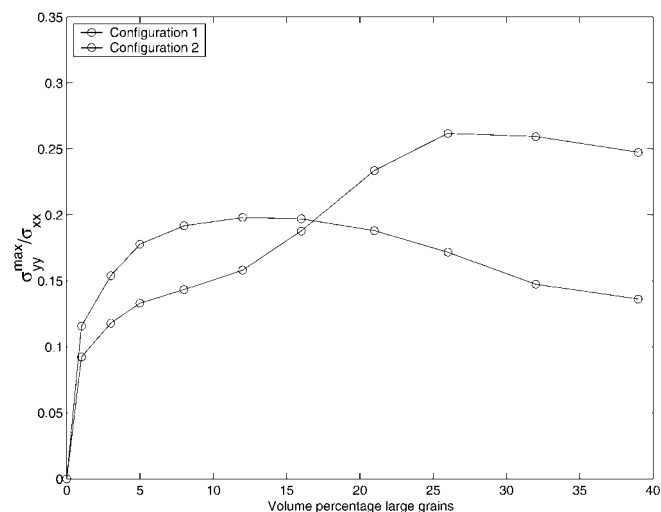


Fig. 10. Maximum σ_{yy} normalized against average stress, $\bar{\sigma}_{xx}$, for different volume percentages of large grains for the two different configurations when loaded by an average strain $\bar{\epsilon}_{xx}$ of 5%.

- Thirdly, the volume fraction of large grains is most important in determining the material properties, not the shape and configuration of the ellipses.

- [1] H. V. Atkinson, *Acta Metall.* **1988**, 36, 469.
- [2] A. C. F. Cocks, S. P. A. Gill. *Acta Mater.* **1996**, 44, 4765.
- [3] D. Fan, L.-Q. Chen, *Acta Mater.* **1997**, 45, 611.
- [4] E. A. Holm, N. Zacharopoulos, D. J. Srolovitz, *Acta Mater.* **1998**, 46, 953.
- [5] S. Zajac, J. Komenda, *Technical Report SIMR/R-99/0-SE*, Swedish Institute for Metals, **1999**.
- [6] F. G. Rammerstorfer, F. D. Fischer, H. J. Böhm, W. Daves, *Comput. Struct.* **1992**, 44, 453.
- [7] E. Werner, T. Siegmund, F. D. Fischer, *Comput. Mater. Sci.* **1994**, 3, 279.
- [8] T. Siegmund, E. Werner, F. D. Fischer, *J. Mech. Phys. Solids* **1995**, 43, 495.
- [9] H. J. Böhm, F. G. Rammerstorfer, F. D. Fischer, T. Siegmund, *J. Eng. Mater. Technol.* **1994**, 116, 268.
- [10] Hibbitt, Karlsson & Sorensen, Inc, Pawtucket, RI, USA. ABAQUS 5.8, **1998** edition.

Degradation of Mechanically Fastened Stainless Steel Joint During Repeated Fastening and Unfastening

By Xiangcheng Luo and Deborah D. L. Chung*

Mechanical fastening involves the application of a force to the components to be joined, so as to prevent the components from separating in service.^[1] During repair, maintenance or other operations, unfastening may be needed. Hence, repeated fastening and unfastening may be necessary. By design, the stresses encountered by the components and fasteners are below the corresponding yield stresses, so that no plastic deformation occurs. However, the local stress at the asperities at the interface can exceed the yield stress, thereby resulting in local plastic deformation, as shown for carbon steel fastened joints at a compressive stress of just 7% or less of the yield stress.^[2] The plastic deformation results in changes in the joint interface. This means that the joint interface depends on the extent of prior fastening and unfastening. The joint interface affects the mechanical and corrosion behavior of the joint. This problem is thus of practical importance.

[*] Prof. D. D. L. Chung, Dr. X. Luo
Composite Materials Research Laboratory
State University of New York at Buffalo
Buffalo, NY 14260-4400 (USA)
E-mail: ddlchung@acsu.buffalo.edu

Stainless steel differs from carbon steel in the presence of passive film^[3-19] and in the higher yield stress. The passive film is important to the corrosion resistance of stainless steel. The effect of repeated fastening and unfastening on the passive film is of concern. This paper extends Luo et al.^[2] from carbon steel to stainless steel. Both Luo et al.^[2] and this work use contact electrical resistance measurement to monitor the joint interface in real time during repeated fastening and unfastening.

Tribology is related to the mechanical interaction of materials in contact. The consequence of the interaction can be mechanical deformation, the loss of material, the damage of material, and the change of the interfacial microstructure and composition, as conventionally observed by weight loss measurement, microscopy, and mechanical testing. These methods typically involve observation after rather than during the mechanical interaction, due to the experimental difficulty of observation during the interaction. Observation during the interaction is valuable for detecting the reversible and irreversible effects, whereas observation after the interaction allows detection of irreversible effects only. A non-destructive monitoring technique that provides information in real time during dynamic loading is desirable. Microscopic examination of the interface viewed at the edge cannot effectively provide interfacial information, though it can be non-destructive and be in real time. Microscopic examination of the interface surfaces after separation of the contacting elements can provide microstructural information, but it cannot be performed in real time. A non-destructive method which is amenable to observation during the mechanical interaction is electrical measurement,^[20-25] in this case the measurement of the contact electrical resistance of the interface.

Figure 2 shows the variation in resistance and displacement during cyclic compressive loading at a stress amplitude of 3.5 MPa. In every cycle, the resistance decreased as the compressive stress increased, such that the maximum stress corresponded to the minimum resistance and the minimum stress corresponded to the maximum resistance (Fig. 2a). The maximum resistance (in the unloaded condition) of every cycle decreased upon stress cycling for the first 7 cycles and

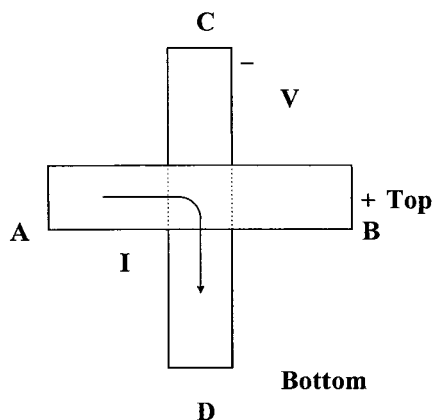


Fig. 1. Steel joint testing configuration.

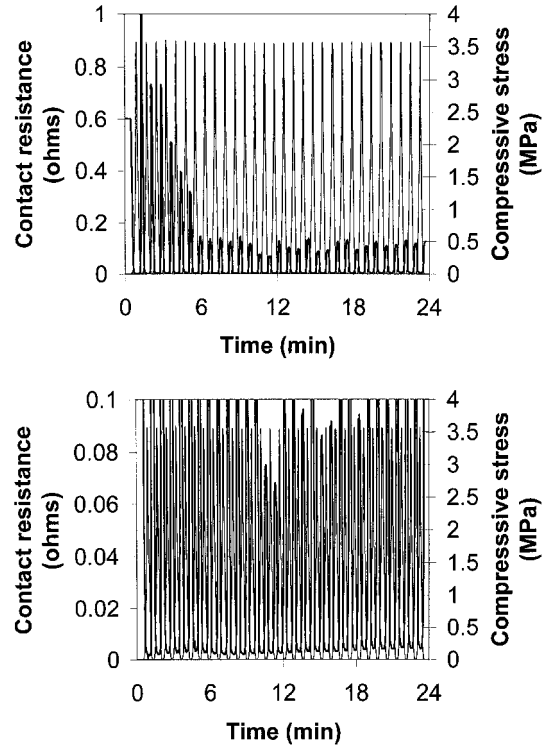


Fig. 2. Variation of contact resistance (thick curve) and stress (thin curve) during cyclic compression at a stress amplitude of 3.5 MPa.

then leveled off (Fig. 2a), due to plastic deformation which was particularly significant during the first few cycles. The minimum resistance (at the maximum stress) of every cycle increased slightly upon cycling (Fig. 2b), probably due to strain hardening at asperities.

Figure 3 shows results obtained during cyclic compressive loading at a stress amplitude of 14 MPa. The maximum resistance (in the unloaded condition) of every cycle increased upon stress cycling, such that the increase was not significant until after 13 cycles (Fig. 3a). The increase is due to the damage of the passive film and the consequent surface oxidation. The minimum resistance (at the maximum stress) of every cycle increased slightly upon cycling (Fig. 4b), probably due to strain hardening.

Figure 4 shows results obtained at a stress amplitude of 28 MPa. The maximum resistance (in the unloaded condition) of every cycle increased upon stress cycling, such that the increase was drastic after about 7 cycles (Fig. 4a). The increase is attributed to passive film damage. The increase was more drastic and occurred earlier in Figure 4 than Figure 3, because of the higher stress amplitude in Figure 4. The minimum resistance (at the maximum stress) of every cycle increased slightly upon cycling, such that the variation was irregular after 8 cycles (Fig. 4b). The irregularity is due to the severe damage of the passive film and the consequent severe oxidation.

The higher the stress amplitude, the fewer is the number of stress cycles for passive film damage to start. At the lowest stress amplitude of 3.5 MPa, passive film damage was not observed up to 30 cycles.

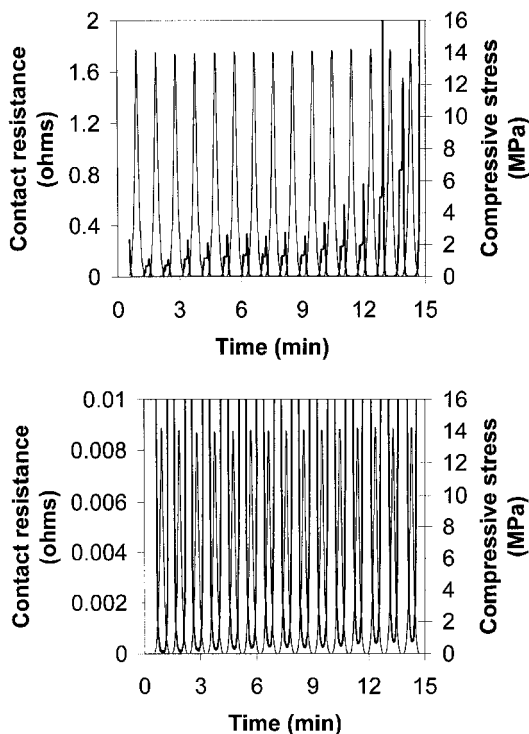


Fig. 3. Variation of contact resistance (thick curve) and stress (thin curve) during cyclic compression at a stress amplitude of 14 MPa.

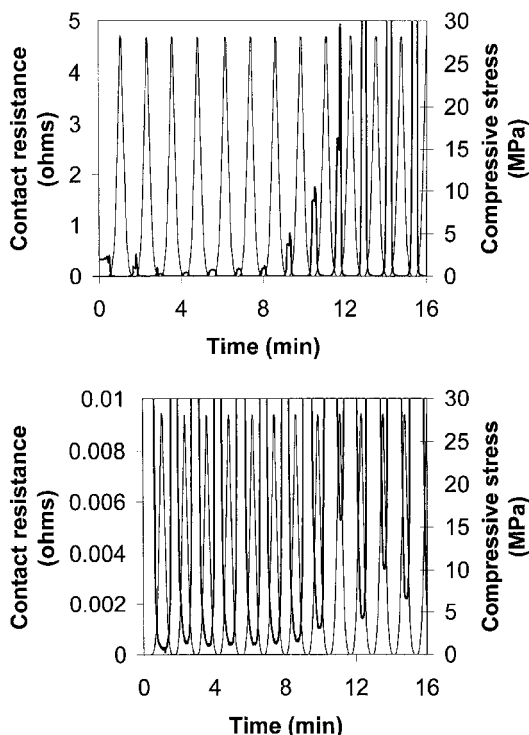


Fig. 4. Variation of contact resistance (thick curve) and stress (thin curve) during cyclic compression at a stress amplitude of 28 MPa.

Comparison of the results of this work on stainless steel and those of Luo et al.^[2] on carbon steel shows that the carbon steel joint is dominated by effects associated with plastic deformation whereas the stainless steel joint is dominated by

effects associated with passive film damage. The effect of the passive film is absent in the carbon steel joint, as expected from the absence of a passive film on carbon steel. The effects of plastic deformation and strain hardening are much larger for carbon steel than stainless steel, as expected from the lower yield stress of carbon steel.

At compressive stresses much below the yield stress, damage of the passive film on stainless steel occurs upon repeated fastening and unfastening of a stainless steel joint. The higher the compressive stress, the more severe is the damage and the fewer is the number of stress cycles it takes for damage to start. The damage leads to surface oxidation, and hence an increase in the contact electrical resistance of the joint interface. Plastic deformation at asperities occurs, but it is less significant than that in a carbon steel joint.

Experimental

The steel used was No.304 stainless steel (annealed, modulus = 193 GPa, tensile yield strength = 330 MPa [26]) that had been mechanically polished by 600 grit sandpaper, in which the average SiC abrasive particle size was 25 μm . Two rectangular strips of stainless steel ($47 \times 11.7 \times 1.40$ mm and $42 \times 11.2 \times 1.40$ mm) were allowed to overlap at 90° to form a nearly square junction (11.7×11.2 mm), as illustrated in Figure 1. The junction was the joint under study. Uniaxial compression (corresponding to the fastening load) was applied at the junction in the direction perpendicular to the junction, using a screw-action mechanical testing system (Sentech 2/D, Sintech, Research Triangle Park, NC), while the contact electrical resistivity of the junction was measured. To measure the contact resistivity, a direct current (DC) was applied from A to D, so that the current traveled down the junction from the top steel strip to the bottom strip. At the same time, the voltage was measured between B and C using a Keithley 2002 multimeter; this voltage was the voltage across the junction between the top and bottom strips. The use of two current probes (A and D) and two voltage probes (B and C) corresponds to the four-probe method of resistance measurement. The voltage divided by the current yielded the contact resistance of the junction. This resistance, multiplied by the junction area, gave the contact resistivity, which is a quantity that is independent of the area of the junction.

Received: March 14, 2000

Final version: August 24, 2000

- [1] M. Diamond, *Sheet Met. Ind.* **1989**, 66, 587.
- [2] X. Luo, D. D. L. Chung, *J. Mater. Eng. Perf.* **2000**, 9, 95.
- [3] J. Zhang, J. Chen, Y. Qiao, C. Cao, *Trans. Inst. Met. Finishing* **1999**, 77, 106.
- [4] A. A. Ono, T. Shinohara, S. Tsujikawa, *Zairyo to Kankyo/Corros. Eng.* **1999**, 48, 169.
- [5] T. Shibata, O. Yamazaki, S. Fujimoto, *Zairyo to Kankyo/Corros. Eng.* **1999**, 48, 155.
- [6] V. Vignal, J. M. Olive, D. Desjardins, *Corros. Sci.* **1999**, 41, 869.
- [7] M. F. Lopez, A. Gutierrez, C. L. Torres, J. M. Bastidas, *J. Mater. Res.* **1999**, 14, 763.
- [8] S. V. Phadnis, M. K. Totlani, D. Bhattacharya, *Trans. Inst. Met. Finishing, Part 6* **1998**, 76, 235.
- [9] N. E. Hakiki, M. Da Curha Belo, A. M. P. Simoes, M. G. S. Ferreira, *J. Electrochem. Soc.* **1998**, 145, 3821.
- [10] M. Lakatos-Varsanyi, F. Falkenberg, I. Olefjord, *Electrochim. Acta* **1998**, 43, 187.

- [11] J. M. Bastidas, M. F. Lopez, A. Gutierrez, C. L. Torres, *Corros. Sci.* **1998**, *40*, 431.
- [12] R. A. Guidotti, G. C. Nelson, *Mater. Res. Soc. Symp. Proc.* **1998**, *496*, 469.
- [13] A. Hannani, F. Kermiche, *Trans. Inst. Met. Finishing, Part 3* **1998**, *76*, 114.
- [14] S. Fujimoto, T. Yamada, T. Shibata, *J. Electrochem. Soc.* **1998**, *145*, L79.
- [15] A. Atrens, B. Baroux, M. Mantel, *J. Electrochem. Soc.* **1997**, *144*, 3697.
- [16] G. Chen, C. R. Clayton, *J. Electrochem. Soc.* **1997**, *144*, 3140.
- [17] F. Mansfeld, C. B. Breslin, A. Pardo, F. J. Perez, *Surf. Coat. Technol.* **1997**, *90*, 224.
- [18] M. Drogowska, H. Menard, A. Lasia, L. Brossard, *J. Appl. Electrochem.* **1996**, *26*, 1169.
- [19] T. J. McKrell, J. M. Galligan, *Mater. Res. Soc. Symp. Proc.* **1996**, *404*, 199.
- [20] C. C. Chou, J. F. Lin, *Proc. Inst. Mech. Eng., Part J: J. Eng.* **1997**, *211*, 209.
- [21] C. Ackerman, H. Lentz, W. Powers, Jr., T. Jones, A. Casuccio, C. Spangler, P. Fischione, D. File, G. Anderson, H. Breindel, B. Reed, *Automated Torque and Resistance Measurements of Sliding Electrical Contacts During Life Testing*, Proc. 36th Annual IEEE Holm Conference on Electrical Contacts **1990**, Illinois Inst. Of Technology, Chicago, IL, pp. 259–268.
- [22] S. J. N. Goodman, T. F. Page, *Wear* **1989**, *131*, 177.
- [23] B. I. Kostetskii, B. V. Gupka, V. E. Gorbanevskii, A. I. Gupka, *Sov. Eng. Res.* **1988**, *8*, 13.
- [24] L. J. Bredell, L. B. Johnson, Jr., D. Kuhlmann-Wilsdorf, *Wear* **1987**, *120*, 161.
- [25] A. P. Braginskii, D. G. Evseev, A. K. Zdan'ski, N. P. Kukol, *Sov. J. Friction Wear (Engl. Transl. of Trenie i Iznos)* **1985**, *6*, 31.
- [26] *Stainless Steels* (Ed: J. R. Davis), ASM Int., Materials Park, OH **1994**.

Measuring Magnetic Susceptibility of Undercooled Co-Based Alloys with a Faraday Balance**

By Sven Reutzel and Dieter M. Herlach*

As a usual experimental experience the existence of magnetic long-range order is limited to the solid state of matter. The Curie temperature, T_C , which signifies the transition from a magnetically ordered ferromagnetic state to a disordered paramagnetic state is much lower than the corresponding melting temperature, T_M , in all metallic elements and alloys. In Co-based alloys of high Curie temperature undercooling to T_C has been shown. Provided heterogeneous nucleation on crucible walls can be eliminated it is well established that metallic melts can be undercooled far below their melting temperature.^[1]

In the past electromagnetic levitation has often been used to undercool liquid metals (e.g. Co–Pd alloys) near to the Curie temperature of the solid α -phase.^[2] This alloy was selected for studies because it shows the highest relative Curie temperature, $T_{rc} = T_C/T_M$, and because the Co–Pd system is completely miscible over the entire concentration range. Confusion due to chemical clustering, as observed in eutectic alloys^[3], for example, and its possible consequences on magnetism of melts^[4] can thus be excluded. While reducing the temperature an attractive force between the Co–Pd sample and an external CoSm permanent magnet was observed, which may indicate the existence of a metallic liquid showing magnetic ordering, as is shown in Figure 1.

As mentioned above, the magnetization of liquid Co-based alloys rises steeply if temperature approaches the Curie temperature, T_C . While using a modified Faraday balance the magnetization has been measured for some Co-based alloys in the liquid state as a function of alloy system and concentration.^[5] This method uses levitation processed samples and indicates general magnetic behavior in the undercooled liquid. The results show that the magnetic susceptibility of the liquid undercooled samples follows Curie–Weiss behavior, from which Curie temperatures are inferred. Figure 2 presents the reciprocal magnetic susceptibility as a function of

[*] S. Reutzel, Prof. D. M. Herlach
DLR, Institute of Space Simulation
D-51170 Köln (Germany)
E-mail: sven.reutzel@dlr.de

[**] The authors acknowledge helpful discussions with W. Bender and thank Prof. B. Feuerbacher for continuous support. This work is financially supported by the German Science Foundation, DFG, within the key-point "Unterkühlte Metallschmelzen".